Eur Biophys J (2010) 39:623–630
DOI 10.1007/s00249-009-0513-2

ORIGINAL PAPER

Solution NMR mapping of water-accessible residues in the transmembrane β-barrel of OmpX

Laurent J. Catoire · Manuela Zoonens · Carine van Heijenoort · Fabrice Giusti · Éric Guittet · Jean-Luc Popot

Received: 4 May 2009 / Revised: 19 June 2009 / Accepted: 22 June 2009 / Published online: 29 July 2009

Abstract The atomic structure of OmpX, the smallest member of the bacterial outer membrane protein family, has been previously established by X-ray crystallography and NMR spectroscopy. In apparent conflict with electrophysiological studies, the lumen of its transmembrane β-barrel appears too tightly packed with amino acid side chains to let any solute flow through. In the present study, high-resolution solution NMR spectra were obtained of OmpX kept water-soluble by either amphipol A8-35 or the detergent dihexanoylphosphatidylcholine. Hydrogen/deuterium exchange measurements performed after prolonged equilibration show that, whatever the surfactant used, some of the amide protons of the membrane-spanning region exchange much more readily than others, which likely reflects the dynamics of the barrel.

The more you see: Spectroscopy in molecular biophysics.

Electronic supplementary material The online version of this article (doi:10.1007/s00249-009-0513-2) contains supplementary material, which is available to authorized users.

L. J. Catoire (✉) · M. Zoonens · F. Giusti · J.-L. Popot
Laboratoire de Physico-Chimie Moléculaire des Protéines Membranaires, UMR 7099,
CNRS/Université Paris-7,
Institut de Biologie Physico-Chimique (FRC 550),
13 rue Pierre et Marie Curie, 75005 Paris, France
e-mail: laurent.catoire@ibpc.fr

C. van Heijenoort · É. Guittet
Laboratoire de Chimie et Biologie Structurales,
ICSN, UPR 2301, CNRS,
91198 Gif-sur-Yvette, France

Keywords Amphipol A8-35 · Hydrogen/deuterium exchange · Membrane protein · OmpX · Surfactant

Introduction

Time-averaged atomic structures of proteins often leave it uncertain how they achieve some of their functions. Outer membrane protein X (OmpX) from *Escherichia coli* is a case in point. While electrophysiological studies suggest that OmpX can translocate ions (Dupont et al. 2004; Arnold et al. 2007), structural studies describe this protein as a rigid transmembrane (TM) β-barrel, whose lumen is too densely packed with amino acid side chains to admit any solute (Vogt and Schulz 1999; Fernández et al. 2001). However, low energy, ground-state conformations do not preclude the existence of time-dependent conformational fluctuations that may allow the transient formation of a channel. In the present study, OmpX kept water-soluble either by amphipol A8-35 or by the detergent dihexanoylphosphatidylcholine (DHPC) was studied by solution NMR. The solvent accessibility of amide protons ($^1H^N$) was investigated by measuring the extent of hydrogen/deuterium (H/D) exchange after extensive equilibration, providing insights into the dynamics of the β-barrel.

Methods

APol synthesis

Fully protonated APol A8-35 (batch FGH20) was obtained by grafting octylamine and isopropylamine groups onto a poly(acrylic acid) precursor (Tribet et al. 1996; Gohon et al. 2004).

Protein expression and purification

Overexpression of uniformly ^{2}H,^{13}C,^{15}N-labeled OmpX (H100N) ([u-^{2}H,^{13}C,^{15}N]OmpX) in *E. coli* using D_2O-based minimal growth media ($^{2}H > 99\%$) with 2 g/l [^{2}H,^{13}C]-D-glucose ($^{2}H > 97\%$, $^{13}C > 98\%$) and 1 g/l $^{15}NH_4Cl$ ($^{15}N > 99\%$) and purification of inclusion bodies (in H_2O solutions) were similar to procedures already described (Vogt and Schulz 1999; Fernández et al. 2001). All isotopically enriched compounds were purchased from Spectra Stable Isotopes (Columbia, MD, USA). The ^{13}C label was introduced in view of other investigations (Catoire et al. 2009). The percentage of deuteration of OmpX was estimated to be ~99% on the basis of mass-spectroscopy measurements, assuming the protein to be labeled to 99% with ^{15}N and ^{13}C (Catoire et al. 2009). Inclusion bodies were solubilized in 6 M urea, 20 mM Tris–HCl, 5 mM EDTA, pH 8.5. OmpX was refolded by slow dilution (Fernández et al. 2001) into a solution of *n*-octylpolyoxyethylene (C_8POE, Bachem) in H_2O. The final protein concentration was 0.3 g/l in 1.5% (w/v) C_8POE.

Preparation of NMR samples

Starting from OmpX solubilized in C_8POE, the following NMR samples were prepared: [u-^{2}H,^{13}C,^{15}N]OmpX in dihexanoylphosphatidylcholine (DHPC) (Avanti Polar Lipids) solution and [u-^{2}H,^{13}C,^{15}N]OmpX trapped by APol A8-35. The OmpX/DHPC sample was prepared as follows. OmpX/C_8POE was diluted 6× with a 2% (w/v) DHPC solution in H_2O (20 mM phosphate buffer, 100 mM NaCl, 0.05% NaN_3, pH 6.8 or pH 8.0) at 4°C. The final C_8POE concentration was 0.3% (w/v), i.e., half the critical micellar concentration. The solution was gently stirred for 3 h and then dialyzed for 30 min at 4°C against the dilution buffer without DHPC. In order to remove any traces of C_8POE, we performed 10 cycles of dilution/concentration in an Amicon centrifugal filter unit (10 kDa cutoff, Millipore) with a 20 mM phosphate buffer, 100 mM NaCl, 0.05% NaN_3 (pH 6.8 or 8.0) in 5% D_2O. The final concentration of the NMR sample was 0.7 mM OmpX. The detergent concentration was adjusted to 200 mM DHPC by adding solid DHPC to the solution, the final concentration being checked by analyzing 1D ^{1}H-NMR spectra, as reported in (Fernández et al. 2001). OmpX trapping by APol was performed as reported for the TM domain of OmpA (Zoonens et al. 2005) at a 1:4 protein/APol ratio (w/w). The final OmpX/APol NMR samples contained either 1.1 mM (in 5% D_2O) or 1.3 mM (in 100% D_2O) [u-^{2}H,^{13}C,^{15}N] OmpX/APol in 20 mM phosphate buffer, 100 mM NaCl, 10 mM EDTA-d_{16} ($^{2}H > 98\%$, CDN isotopes), 0.05% NaN_3, pH ~8.0. The folding of OmpX in H_2O and subsequent transfer to DHPC or APol in either 5 or 100% D_2O solutions took place on the same day. H_2O/D_2O exchange was carried out on Amicon ultracentrifugal devices with a 10-kDa molecular weight cutoff (MWCO) (Millipore). Ten cycles of concentration/dilution with 100% D_2O solutions were performed, amounting to an H_2O dilution factor of 6^{10} (i.e., $[H_2O]_{residual} \leq 1$ μM). The samples were then stored at 4°C for 8 weeks prior to NMR experiments. The final APol concentration was estimated on the basis of the initial amount added, since A8-35 molecules, whether part of OmpX/APol complexes or present as free particles (~40 kDa; see ref. Gohon et al. 2006), are unable to cross the Amicon filters.

NMR spectroscopy

All NMR experiments with OmpX were carried out at 30°C on a Bruker Avance II 700 spectrometer equipped with a 5-mm triple-resonance (TXI) gradient probe. The following parameters were used for each type of experiment: 2D [^{15}N,^{1}H] transverse relaxation-optimized spectroscopy (TROSY) (Pervushin et al. 1997) and heteronuclear single quantum coherence (HSQC) experiments [data size $128(t_1) \times 2{,}048(t_2)$ complex points, $t_{1_{max}}(^{15}N) = 56$ ms, $t_{2_{max}}(^{1}H) = 244$ ms]; 1D [^{15}N,^{1}H]-TROSY rotational correlation time (TRACT) experiment (Lee et al. 2006) [2,048 complex points, $t_{1_{max}} = 213$ ms, relaxation delay $(\Delta_i) = 2$ to 150 ms, 2,048 transients per Δ_i]. Chemical shifts are referenced to an internal standard of 2,2-dimethyl-2-silapentane-5-sulfonate sodium salt (DSS). Chemical shift assignments are based on those available for OmpX/DHPC complexes (BMRB Entry 4936). Samples of OmpX in DHPC at both pH 6.8 and 8.0 were used to assign peaks in the TROSY spectrum of OmpX/APol complexes. Any correlation peak whose assignment was uncertain—especially for residues belonging to the extracellular loops or protruding part of some β-sheets—was excluded from the analysis. The TROSY experiment was repeated three times per sample and peak volumes were averaged. Data processing was performed with NMRPipe software (Delaglio et al. 1995) and spectra analyzed with NMRView (Johnson and Blevins 1994). The protection factor ε_{eq} represents the ratio of peak volumes for OmpX/APol complexes incubated in 100 versus 5% D_2O. ε_{eq} is normalized relative to the ratio observed for the most protected residue.

Results and discussion

Characterization of OmpX/APol versus OmpX/detergent complexes

Amphipols (APols) are short amphipathic polymers used as milder substitutes for detergents (Tribet et al. 1996; Popot et al. 2003). They keep membrane proteins (MPs) water-

soluble by adsorbing onto their transmembrane (TM) surface (Zoonens et al. 2005; Catoire et al. 2009). Complexes between MPs and APol A8-35 (Fig. 1a) can be studied by solution NMR provided the pH is >7 (Zoonens et al. 2005; Catoire et al. 2009). In keeping with observations on other membrane proteins (see, e.g., Zoonens et al. 2005; Gohon et al. 2008), 2D [^{15}N,^{1}H]-TROSY (Pervushin et al. 1997) spectra (Fig. 1b) show that OmpX in A8-35 is correctly folded. Indeed, except for the loss of correlation peaks for some residues located in the loops due to faster chemical exchange with the solvent at high pH, spectra collected in A8-35 at pH 8.0 and in the detergent DHPC at pH 6.8 are very similar (Fig. 1b). In particular, the glycine resonances (upfield in the ^{15}N dimension) and the β-sheet peaks (downfield in the ^{1}H dimension) have nearly the same chemical shifts in the two environments. This indicates identical secondary and tertiary structures whether the protein is complexed by APols or kept in detergent solution.

The average line width in the direct dimension increases from 20.2 ± 2.4 Hz (SD) in DHPC to 27.0 ± 3.1 Hz in APol (in the presence of EDTA). The slightly larger size of OmpX/A8-35 versus OmpX/DHPC particles is reflected in their effective rotational correlation times (τ_c): $\tau_c = 31 \pm 4$ ns at 30°C for OmpX/A8-35 complexes (Fig. 2) versus 23 ± 2 ns for OmpX/DHPC complexes (Fernández et al. 2001). The presence of EDTA in OmpX/A8-35 samples substantially reduces the line width, by about one-third on average (ca. −13 Hz). EDTA likely prevents the formation of interparticle bridges resulting from the interaction of APol A8-35 carboxylate groups with traces of multivalent cations. Hence, the difference in size between OmpX/A8-35 and OmpX/DHPC complexes appears much reduced compared to previous investigations carried out on the TM domain of OmpA in the absence of EDTA (Zoonens et al. 2005). Working at pH > 7 remains a disadvantage, however, since it leads to the loss or broadening of many correlation peaks originating from solvent-exposed

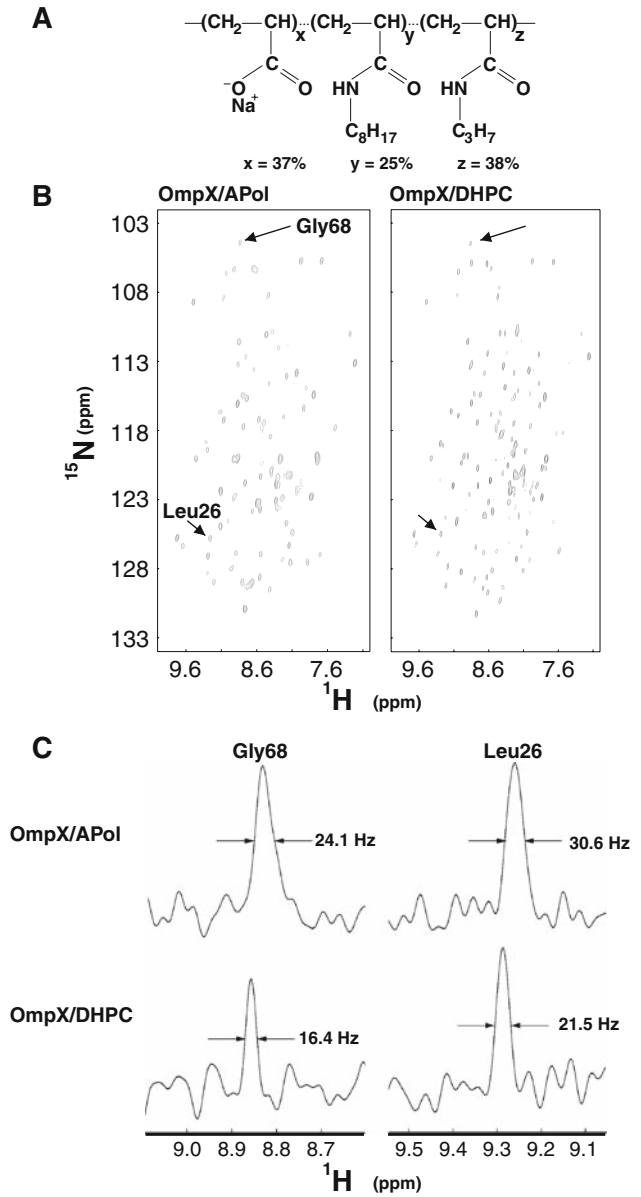

Fig. 1 **a** Chemical structure of A8-35, a polyacrylate-based APol (Tribet et al. 1996). The average degree of polymerization is ~70, the average molecular weight ~9 kDa. The molar percentage of each type of unit (*x*, *y*, and *z*), randomly distributed along the chain, is indicated for batch FGH20. **b** 2D [^{15}N,^{1}H]-TROSY spectra of [u-^{2}H,^{13}C,^{15}N]OmpX complexed by A8-35 (*left* [OmpX] = 1.3 mM, 8 transients/increment, pH 8.0) or by DHPC (*right* [OmpX] = 0.7 mM, 16 transients/increment, pH 6.8). **c** Cross-sections of two selected resonance peaks. The *upper and lower rows* are taken from the left and right spectra of **b**, respectively

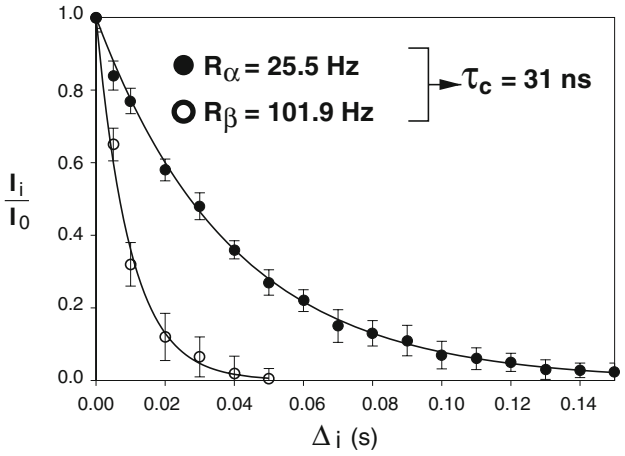

Fig. 2 Effective correlation time, τ_c, of [u-^{2}H,^{13}C,^{15}N]OmpX/APol complexes estimated by a 1D [^{15}N,^{1}H]-TROSY rotational correlation time (TRACT) experiment (Lee et al. 2006). I_0 and I_i are integrations of the $^{1}H^{N}$ 1D spectrum region at $t = 0$ and $t = \Delta_i$, respectively. The *upper and lower curves* correspond to the slow (α-spin state of ^{15}N) and fast (β-spin state of ^{15}N) transverse relaxation decays. The exponential fits yield the R_α and R_β values indicated, from which an estimate of τ_c can be derived as described in Lee et al. (2006)

residues. This may hopefully be alleviated in the future through the use of pH-insensitive APols, currently under development (Diab et al. 2007; Sharma et al. 2008; Dahmane et al., unpublished). In the present work, we have focused on poorly accessible, slowly exchanging TM amide protons.

H/D exchange measurements

The accessibility of $^{1}H^{N}$ protons involved in the β-barrel hydrogen bond network was assessed by comparing [^{15}N,^{1}H]-TROSY spectra collected after extensive equilibration (8 weeks at 4°C) of OmpX/A8-35 complexes in either 5 or 100% D_2O (Fig. 3). Unsurprisingly, the most protected $^{1}H^{N}$ protons (in red in Fig. 4b) are found in the TM region of the barrel, with a few residues at both ends of each strand showing higher accessibility; the protection factor (ε_{eq}) of the latter can be 30 to 50% lower than that of residues located towards the center of the TM region, if not null (Fig. 4; see also Table S1 in Supplementary Material). The number of protected $^{1}H^{N}$ protons differs among β-strands, the first two strands, in particular, displaying only a few partially shielded $^{1}H^{N}$ protons towards the midst of the transmembrane region. Interestingly, these more accessible strands comprise the most highly conserved sequence segments in the family of eight-stranded OMPs (Baldermann et al. 1998) (Fig. 4b).

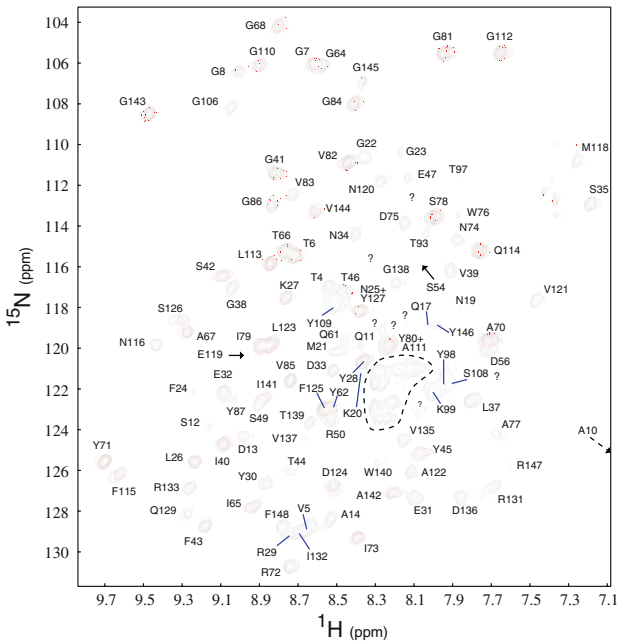

Fig. 3 Superimposed 2D [^{15}N,^{1}H]-TROSY spectra of [u-^{2}H,^{13}C,^{15}N] OmpX complexed by APol A8-35. The sample was prepared in D_2O and stored at 4°C either in 5% (in *black*, 8 transients/increment) or in 100% D_2O (in *red*, 128 transients/increment) for 8 weeks before NMR experiments. The *dashed line* delineates a crowded area including correlations peaks of residues Y9, Q15, Y57, N58, K59, N60, Y63, Q91, E94, D101, and D104

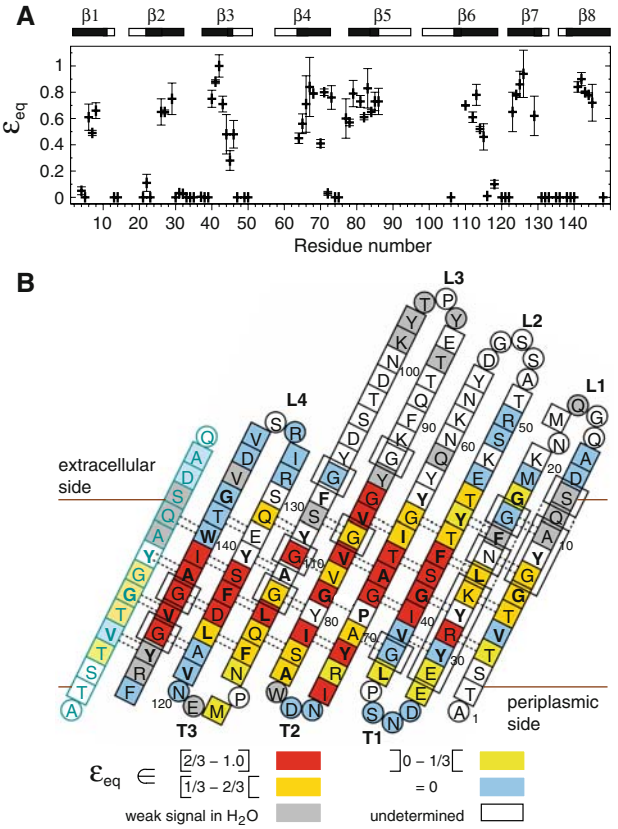

Fig. 4a, b Solvent accessibility of amide ^{1}H revealed by H/D exchange. **a** $^{1}H^{N}$ protection factor ε_{eq} plotted against residue number. ε_{eq} represents the ratio of peak volumes for OmpX/APol complexes incubated in 100 versus 5% D_2O (data from the TROSY spectra shown in Fig. 2). ε_{eq} is normalized relative to the ratio observed for the most protected residue, S42. The position of β-strands is indicated by *bars* above the graph, with *black and white* sections noting the TM and extramembrane regions, respectively. **b** Topology diagram of the protein. Residues belonging to the β-barrel are shown in *squares*, with *bold letters* indicating that the side chain points towards the surfactant. Hydrogen bonds in the TM region are indicated by *dotted lines*. High homology sequences and conserved residues in the eight-stranded β-barrel family are framed by a *solid line*. *Colors* refer to ranges of ε_{eq}. *Colorless* residues are prolines or residues for which $^{1}H^{N}$ and ^{15}N chemical shifts are not known, residues that were not unambiguously assignable in the OmpX/APol spectrum due to chemical shift differences with the spectrum in DHPC, overcrowding of the lines, and/or lines that were too broadened by the high pH (residues belonging to the loops or to the protruding part of β-strands), or residues with indistinguishable $^{1}H^{N}/^{15}$N chemical shifts. Residues whose correlation peaks are too weak in H_2O to permit a reliable estimation of ε_{eq} are shown in *gray*

H/D exchange measurements carried out in DHPC at pH 8.0 yielded essentially the same results (data in red in Figs. 5, 6a, 7; see also SM Fig. S1, Table S2). Comparison of absolute peak intensities after incubation in 100 versus 5% D_2O shows that, both in A8-35 and in DHPC, some protons do not exchange at all, including those taken as

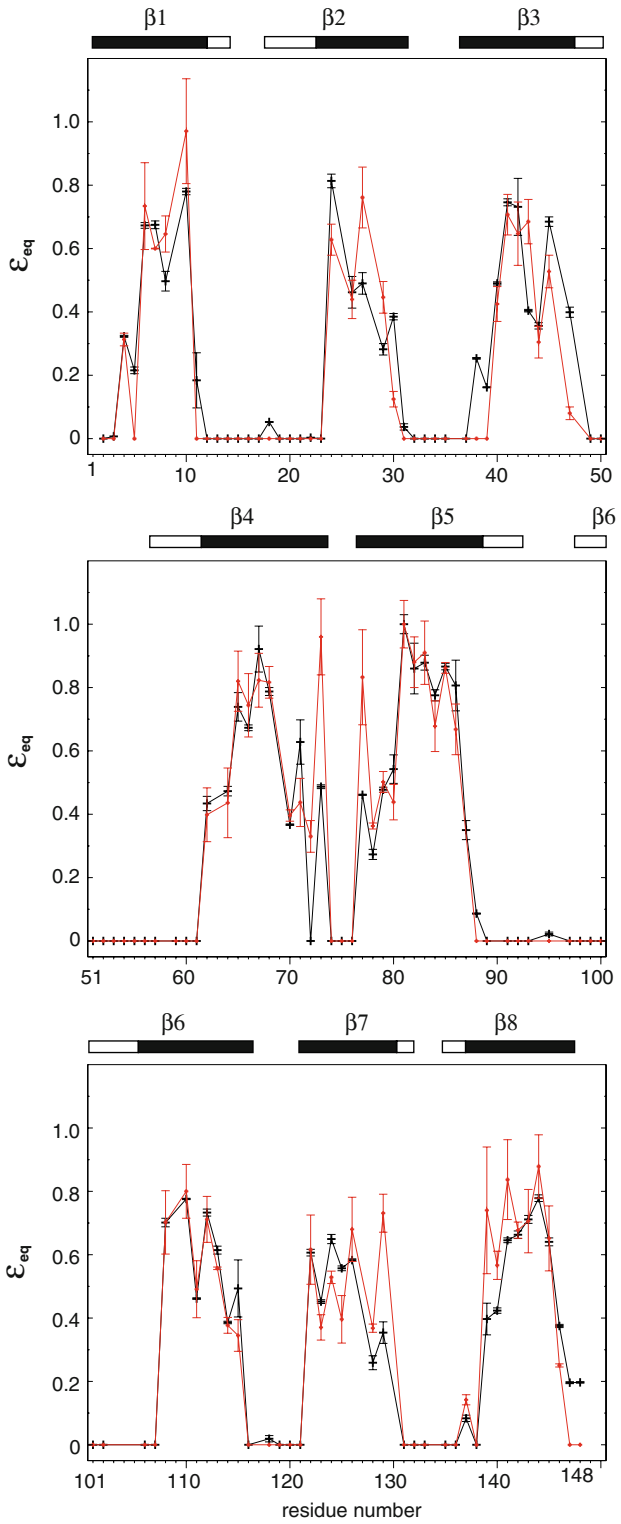

Fig. 5 Influence of pH on $^1H^N$ solvent accessibility of OmpX in DHPC solution. $^1H^N$ protection factors ε_{eq} plotted against residue number obtained at pH 6.8 (*black*) and 8.0 (*red*). ε_{eq} is normalized relative to the ratio observed for the most protected residue, that is, at both pH values, G81

references for the calculation of ε_{eq}. Most of those that do exchange do it to comparable degrees in the two environments (Fig. 7), suggesting that the overall dynamics of the barrel remains the same. As in A8-35, amide protons in the TM region of OmpX/DHPC complexes display variable ε_{eq} values. In DHPC, except for strands 4 and 5, residues belonging to the end of the barrel that faces the periplasmic space tend to exchange somewhat more than in A8-35 (Figs. 4b, 5, 6b). Differences of ε_{eq} values between samples in DHPC and in A8-35, however, generally do not exceed the ±0.3 range (Fig. 7), which is similar to the deviation observed between duplicate measurements performed in the same medium (Figs. 4a, 5). Some larger differences nevertheless can be detected. The amide protons of residues A122, T139, and W140, for instance, exchange significantly more readily in OmpX/APols complexes than in OmpX/DHPC ones (Fig. 7).

Changing the pH of the solution from 8.0 to 6.8 affects the extent of $^1H^N$ exchange within the TM barrel of DHPC-solubilized OmpX (Figs. 5, 6; see also SM Figs. S1, S2 and Tables S2, S3). On average, the peak volumes in D_2O are 70% lower at pH 8 than at pH 6.8, illustrating the difference in exchange rate. In relative terms, the periplasmic end of the *β*-barrel displays higher ε_{eq} values at pH 6.8 than at pH 8, but there are important local variations. For instance, strands 4 and 5 evolve in the opposite direction, with substantially lower ε_{eq} values for residues I73 and A77 (Fig. 5). The extracellular ends of the TM region of strands 7 and 8 show an increased relative degree of exchange (residues E128, Q129, V137, T139, W140, I141, and A142), as do the $^1H^N$ protons of residues K27, R29, and F43 (mid-TM region of strands 2 and 3). The higher protection factors observed for some residues at lower pH is the expected consequence of slower chemical exchange. On the other hand, when an opposite effect is observed, as is the case, for instance, for residues I73 and A77, an increased accessibility to water at pH 6.8 appears the most likely cause. This could originate from a modification of either the structure or the dynamics of the *β*-barrel upon changing the pH.

Existing data on the structure and dynamics of OmpX shed little light on the nature of the structural fluctuations that lead to $^1H^N$ exchange. On a fast dynamic timescale (ps, ns), fluctuations in the TM part of *β*-strands have been detected in OmpX/DHPC complexes through $^{15}N\{^1H^N\}$-nuclear overhauser effect (NOE) relaxation measurements (Fernández et al. 2004). They show modest differences from strand to strand, which are difficult to correlate with the present data. Molecular dynamics (MD) simulations carried out for up to 100 ns on OmpX/DHPC complexes show fluctuations of amino acid side chains pointing into

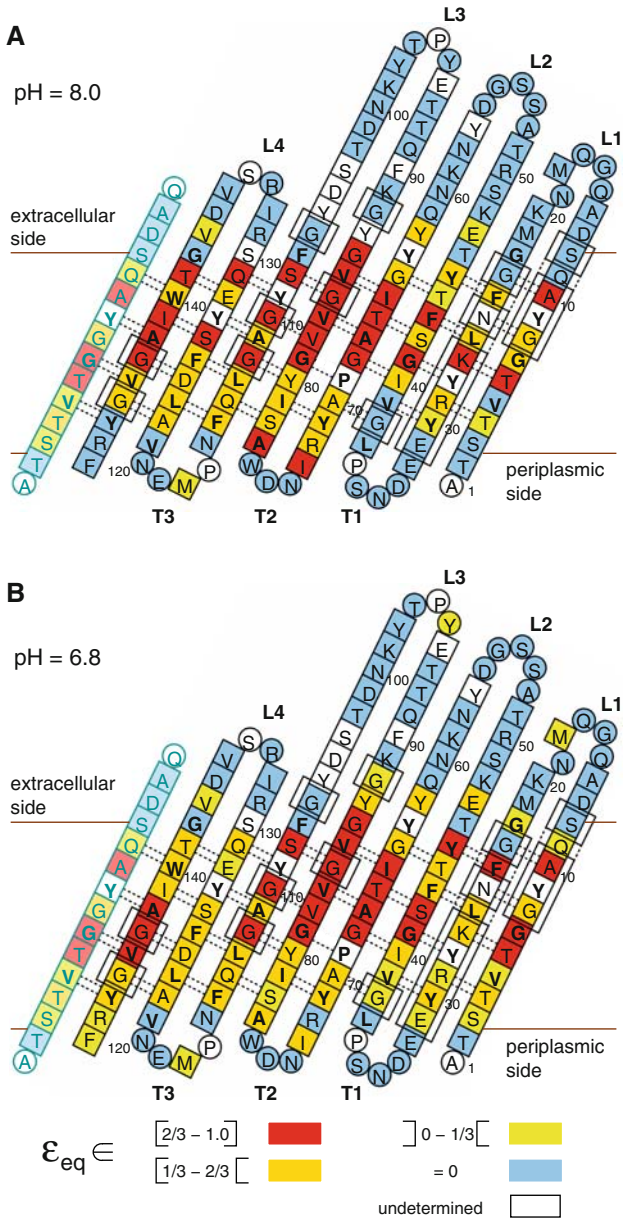

Fig. 6 $^{1}H^{N}$ protection factors ε_{eq} in DHPC at pH 8.0 (*top*) or 6.8 (*bottom*) (from Fig. 5) represented on topology diagrams of the protein. Residues are color-coded as a function of ε_{eq} values according to the code defined in Fig. 4

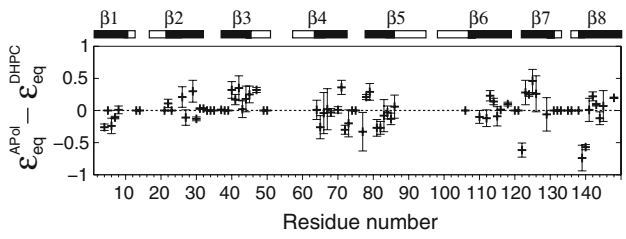

Fig. 7 Comparison of $^{1}H^{N}$ protection factors observed at pH 8 with OmpX in complex with APol A8-35 or solubilized by DHPC

the barrel, but, on this timescale, no ion or water permeation (Böckmann and Caflisch 2005; Cox et al. 2008). There is a good correlation between MD and NOE data, as well as X-ray temperature factors, as far as the relative mobility of strands and loops is concerned (see Fig. 2c in Böckmann and Caflisch 2005). None of these data, however, would reveal rare events such as those that may give rise to H/D exchange within the TM region of β-strands over the very long timescale (8 weeks) of the present experiments.

Whatever the exact mechanism by which some of the TM amide protons exchange with the solution, our observations show that the barrel does not behave as a solid block, some of its strands appearing more mobile (and/or accessible) than others. While it cannot be excluded that the water molecules involved in the exchange originate from within the surfactant layer, they may well come from the lumen of the barrel. H/D exchange, in this hypothesis, would provide insights into conformational changes that affect the packing of side chains in the lumen. One interesting working hypothesis could be that ion flux is associated with small relative movements of strands 1 and 2 that would free the side chain of K27—a well-conserved residue of strand 2 with relatively accessible hydrogen bonds to strand 1 (see Fig. 3b). This could result in the disruption of the intraluminal network of hydrogen bonds in which the polar group of K27 is involved (see Böckmann and Caflisch 2005), letting a transient channel form. A similar channel-gating mechanism has been proposed for OmpA (Hong et al. 2006a).

On the other hand, the dynamics of the β-strands suggested by H/D exchange measurements could reflect a transport mechanism distinct from ion flux. Recently, a lateral diffusion model for the uptake of hydrophobic substrates has been proposed for the FadL protein family, which comprises bacterial outer membrane proteins whose transmembrane region is made up of a 14-strand β-barrel (Hearn et al. 2009). Lateral opening of the barrel was postulated to allow hydrophobic substrates picked up from the external medium access to the interior of the outer membrane, thus bypassing the hydrophilic barrier opposed by the outer surface of the lipopolysaccharide layer (Hearn et al. 2009). These authors suggested that a similar type of lateral opening could take place in two other, unrelated outer MPs, PagP and OmpW (as regards OmpW, see also Hong et al. 2006b). Like that of OmpX, the transmembrane β-barrels of PagP and OmpW comprise only eight strands and feature a narrow lumen occluded by amino acid side chains (Hwang et al. 2002; Ahn et al. 2004; Hong et al. 2006b). In the structure of OmpW, two neighboring proline residues, one of them highly conserved, seem to induce a gap between two strands, wide enough to allow for the lateral diffusion of small hydrophobic residues into the lipid

bilayer (Hong et al. 2006b). By analogy, one can wonder whether the plasticity of OmpX's transmembrane β-barrel suggested by the present data could not allow it to play a role in the import or export of hydrophobic molecules. OmpX features a proline residue, facing a glycine, in its transmembrane region (P69, Fig. 4). The proline is not strickly conserved (Baldermann et al. 1998), though, and no gap is obvious at the barrel surface in the X-ray and NMR structures (Vogt and Schulz 1999; Fernández et al. 2001). G81, the residue engaged into a hydrogen bond with P69, has a high-protection factor in DHPC whatever the pH, and it is also one of the most protected residues in OmpX/A8-35 complexes ($\varepsilon_{eq} = 0.73$, see SM). Whether these two residues are engaged into a mechanism similar to that postulated for FadL, PagP, and OmpW remains, therefore, highly conjectural. Should OmpX have such a function, however, the transient flow of ions revealed by electrophysiological experiments could well be a consequence rather than the raison d'être of the dynamics of the channel.

In summary, improved experimental conditions (presence of EDTA) have made it possible to record high-resolution NMR data on OmpX complexed by amphipol A8-35. H/D exchange within the TM barrel was studied and compared to that observed with OmpX solubilized in detergent at the same pH (8.0). No substantial differences were observed between the two samples. Hence, the differential rate of exchange between strands revealed by these studies appears to reflect an intrinsic dynamical property of OmpX rather than an effect of its environment. Data obtained with OmpX/DHPC samples further reveal differential variations of the rate of exchange with the pH of the solution. Altogether, the present data suggest that the TM barrel of OmpX presents a certain degree of conformational plasticity, which may possibly account for the protein's hitherto unexplained channel-forming properties. Indeed, should such fluctuations take place in the membrane, they could facilitate the exchange of hydrophobic molecules with the hydrophobic core of the outer membrane, as proposed for FadL (Hearn et al. 2009). Such a transconformation could be accompanied by a modest transient transmembrane flow of ions, as observed experimentally (Dupont et al. 2004; Arnold et al. 2007).

Acknowledgments This work was funded by the CNRS, Paris-7 University, and financial support to J.-L.P. by the HFSP Organization (grant RG00223/2000-M) and the Fondation Rothschild.

References

Ahn VE, Lo EI, Engel CK, Chen L, Hwang PM, Kay LE, Bishop RE, Privé GG (2004) A hydrocarbon ruler measures palmitate in the enzymatic acylation of endotoxin. EMBO J 23:2931–2941

Arnold T, Poynor M, Nussberger S, Lupas AN, Linke D (2007) Gene duplication of the eight-stranded β-barrel OmpX produces a functional pore: a scenario for the evolution of transmembrane β-barrel. J Mol Biol 366:1174–1184

Baldermann C, Lupas A, Lubieniecki J, Engelhardt H (1998) The regulated outer membrane protein Omp21 from *Comamonas acidovorans* is identified as a member of a new family of eight-stranded beta-sheet proteins by its sequence and properties. J Bacteriol 180:3741–3749

Böckmann RA, Caflisch A (2005) Spontaneous formation of detergent micelles around the outer membrane protein X. Biophys J 88:3191–3204

Catoire LJ, Zoonens M, van Heijenoort C, Giusti F, Popot J-L, Guittet É (2009) Inter- and intramolecular contacts in a membrane protein/surfactant complex observed by heteronuclear dipole-to-dipole cross-relaxation. J Magn Reson 197:91–95

Cox K, Bond PJ, Grottesi A, Baaden M, Sansom MS (2008) Outer membrane proteins: comparing X-ray and NMR structures by MD simulations in lipid bilayers. Eur Biophys J 37:131–141

Delaglio F, Grzesiek S, Vuister GW, Zhu G, Pfeifer J, Bax A (1995) NMRPipe: a multidimensional spectral processing system based on UNIX pipes. J Biomol NMR 6:277–293

Diab C, Tribet C, Gohon Y, Popot J-L, Winnik FM (2007) Complexation of integral membrane proteins by phosphorylcholine-based amphipols. Biochim Biophys Acta 1768:2737–2747

Dupont M, Dé E, Chollet R, Chevalier J, Pagès J-M (2004) *Enterobacter aerogenes* OmpX, a cation-selective channel mar- and osmo-regulated. FEBS Lett 569:27–30

Fernández C, Adeishvili K, Wüthrich K (2001) Transverse relaxation-optimized NMR spectroscopy with the outer membrane protein OmpX in dihexanoyl phosphatidylcholine micelles. Proc Natl Acad Sci USA 98:2358–2363

Fernández C, Hilty C, Wider G, Günter P, Wüthrich K (2004) NMR structure of the integral membrane protein OmpX. J Mol Biol 336:1211–1221

Gohon Y, Pavlov G, Timmins P, Tribet C, Popot, J-L, Ebel C (2004) Partial specific volume and solvent interactions of amphipol A8-35. Anal Biochem 334:318–334

Gohon Y, Giusti F, Prata C, Charvolin D, Timmins P, Ebel C, Tribet C, Popot, J-L (2006) Well-defined nanoparticles formed by hydrophobic assembly of a short and polydisperse random terpolymer, amphipol A8-35. Langmuir 22:1281–1290

Gohon Y, Dahmane T, Ruigrok R, Schuck P, Charvolin D, Rappaport F, Timmins P, Engelman DM, Tribet C, Popot J-L, Ebel C (2008) Bacteriorhodopsin/amphipol complexes: structural and functional properties. Biophys J 94:3523–3537

Hearn EM, Patel DR, Lepore BW, Indic M, van den Berg B (2009) Transmembrane passage of hydrophobic compounds through a protein channel wall. Nature 458:367–370

Hong H, Szabo G, Tamm LK (2006a) Electrostatic couplings in OmpA ion-channel gating suggest a mechanism for pore opening. Nat Chem Biol 2:627–635

Hong H, Patel DR, Tamm LK, van den Berg B (2006b) The outer membrane protein OmpW forms an eight-stranded beta-barrel with a hydrophobic channel. J Biol Chem 281:7568–7577

Hwang PM, Choy WY, Lo EI, Chen L, Forman-Kay JD, Raetz CR, Privé GG, Bishop RE, Kay LE (2002) Solution structure and dynamics of the outer membrane enzyme PagP by NMR. Proc Natl Acad Sci USA 99:13560–13565

Johnson BA, Blevins RA (1994) NMRView: a computer program for the visualization and analysis of NMR data. J Biomol NMR 4:603–614

Lee D, Hilty C, Wider G, Wüthrich K (2006) Effective rotational correlation times of proteins from NMR relaxation interference. J Magn Reson 178:72–76

Pervushin K, Riek R, Wider G, Wüthrich K (1997) Attenuated T2 relaxation by mutual cancellation of dipole–dipole coupling and chemical shift anisotropy indicates an avenue to NMR structures of very large biological macromolecules in solution. Proc Natl Acad Sci USA 94:12366–12371

Popot J-L, Berry EA, Charvolin D, Creuzenet C, Ebel C, Engelman DM, Flötenmeyer M, Giusti F, Gohon Y, Hervé P, Hong Q, Lakey JH, Leonard K, Shuman HA, Timmins P, Warschawski DE, Zito F, Zoonens M, Pucci B, Tribet C (2003) Amphipols: polymeric surfactants for membrane biology research. Cell Mol Life Sci 60:1559–1574

Sharma KS, Durand G, Giusti F, Olivier B, Fabiano AS, Bazzacco P, Dahmane T, Ebel C, Popot J-L, Pucci B (2008) Glucose-based amphiphilic telomers designed to keep membrane proteins soluble in aqueous solutions: synthesis and physical–chemical characterization. Langmuir 24:13581–13590

Tribet C, Audebert R, Popot J-L (1996) Amphipols: polymers that keep membrane proteins soluble in aqueous solutions. Proc Natl Acad Sci USA 93:15047–15050

Vogt J, Schulz GE (1999) The structure of the outer membrane protein OmpX from *Escherichia coli* reveals possible mechanisms of virulence. Structure 7:1301–1309

Zoonens M, Catoire LJ, Giusti F, Popot J-L (2005) NMR study of a membrane protein in detergent-free aqueous solution. Proc Natl Acad Sci USA 102:8893–8898